IC/94/69

INTERNATIONAL CENTRE FOR THEORETICAL PHYSICS

FULL MOMENT TENSOR RETRIEVAL AND FLUID DYNAMICS IN VOLCANIC AREAS: THE CASE OF PHLEGRAEAN FIELDS (SOUTH ITALY)

P. Campus

G. Cespuglio

and

G.F. Panza

INTERNATIONAL ATOMIC ENERGY AGENCY

UNITED NATIONS EDUCATIONAL, SCIENTIFIC AND CULTURAL ORGANIZATION

MIRAMARE-TRIESTE

IC/94/69

International Atomic Energy Agency
and
United Nations Educational Scientific and Cultural Organization
INTERNATIONAL CENTRE FOR THEORETICAL PHYSICS

FULL MOMENT TENSOR RETRIEVAL AND FLUID DYNAMICS IN VOLCANIC AREAS: THE CASE OF PHLEGRAEAN FIELDS (SOUTH ITALY)

P. Campus, G. Cespuglio
Istituto di Geodesia e Geofisica, Università degli Studi di Trieste,
via dell'Università 7, 34124 Trieste, Italy

and

G.F. Panza
International Centre for Theoretical Physics, Trieste, Italy
and
Istituto di Geodesia e Geofisica, Università degli Studi di Trieste,
via dell'Università 7, 34124 Trieste, Italy.

MIRAMARE – TRIESTE
April 1994

ABSTRACT

When studying seismicity in volcanic areas it is appropriate to treat the seismic source in a form a priori not restricted to a double couple, since its mechanism may reflect not only small scale tectonics but also fluid dynamics. The monitoring of fluid dynamics can be, therefore, attempted from the retrieval of the rupture processes. To determine the non double-couple components of the seismic source it is not possible to use standard methods, based on the distribution of polarities of first arrivals.

Our new method is based on the wave form inversion of the dominant part of the seismograms, where the signal to noise ratio is very large, and allows us the inversion of the full seismic moment tensor. This tensor is decomposed into a volumetric part (V), representing volume changes, a compensated linear vector dipole part (CLVD), representing lenticular crack activations accompanied by fluid motion, and a double couple (DC) part, representing dislocation movements. The point source approximation is used, and this is justified by the relatively small size of the events that usually occur in volcanic areas. In the inversion, the hypocentral depth and the structural model in which the waves are propagating are not fixed a priori, and each moment tensor component can vary in time, independently from the others; it is, therefore, possible to extract the source time function, even if the mechanism changes in time.

The results of a pilot study in the Phlegraean Fields (South Italy) are presented. Most of the seismic activity characterizing this area is represented by events with relatively low magnitude, in the range from 1 to 3, which can be recorded only by local networks. When a seismic crisis occurs, usually in connection with bradyseism, the number of these events is very large, therefore it is possible to extract from them statistically significant information about the local stress field, and to study in detail the evolution in time of the seismic moment tensor. The application of the new inversion method is particularly appropriate in this area, where the reconstruction of the geometrical part of the moment tensor with the standard methods is generally unreliable, since the low number of recording stations available, and the high level of noise, makes extremely difficult, if not impossible, the use of the polarity of the first arrivals.

INTRODUCTION

Most of the seismicity characterising volcanic and geothermal areas is represented by quite small events, that reflect the local answer to the global tectonic setting. Due to the strong seismic noise encountered in these areas, the source mechanisms of these events are usually very difficult to be studied by standard techniques based on first arrivals, unless a very dense network of seismometers is available. Furthermore when studying volcanic events, it is highly desirable to treat a seismic source in a form not a priori restricted to a double couple because the mechanism may reflect not only the local conditions such as small-scale tectonics, but also fluid motion.

The unconstrained moment tensor description, which permits the decomposition of the full moment tensor solution into a double-couple component (DC), a volumetric component (V), and a compensated linear vector dipole component (CLVD) is, at present, the most suitable approach to study seismic sources in volcanic areas.

The bradyseismic phenomena, accompanied by seismic events, which have occurred in the Phlegraean Fields during the 70ies and 80ies produced an increasing excitation state both in the scientific community and in the common people, since these manifestations let everyone think a possible explosive eruption.

Here we apply the wave form inversion method developed by Sìleny' and Panza (1991) and Sìleny', et al. (1992) which allows us to reconstruct both the geometric (focal mechanism) and the temporal behaviour (source time function) of the unconstrained seismic moment. The data analysed were recorded during the most recent bradyseismic crises, in the years 1984 (ascending bradyseismic phase) and 1986 (descending bradyseismic phase).

THE PHLEGRAEAN FIELDS (P.F.)

The P.F. are one of the classic active volcanic areas of the Quaternary Potassic Roman Province, the volcanic Province of central southern Italy. Since the beginning of their activity (not precisely, but certainly earlier than 50,000 years BP.) the P.F. have been characterised by an impressive series of volcanic eruptions the proximal products of which cover an area of about 200 km² west of Naples.

The caldera is flanked on the east by Mt. Vesuvius and on the west by the volcanic islands of Ischia and Procida. All of these eruptive centres, except Procida, have been active in historic times.

Because of the intense thermal manifestation, frequent earthquakes and vertical ground motion, P.F. are considered as an active volcanic area quiescent since Monte Nuovo eruption (1538), which was preceded by several years of perceived seismicity and by an abrupt uplift of approximately 5 m. In 1982 unrest began which consisted of early chemical changes in the high-temperature fumarolic gases of the Solfatara crater, followed by uplift and then by frequent shallow seismic events (3-5 km maximum hypocentral depth). The crisis went on until the end of 1984, totalling a maximum uplift of 185 cm; since January 1985 the area is slowly deflating (30 cm of deflation by the end of 1986) whereas seismicity stays at very low levels. A similar behaviour, although less documented, has been observed during the 1970-72 unrest (Barberi et al. 1989).

INVERSION OF OBSERVED WAVEFORMS

The method developed by Sìleny' and Panza (1991) and Sìleny' et al. (1992) is applied to seismograms recorded in the P.F. during two bradyseismic crises: the ascending phase of 1984 and the descending one of 1986.

This waveform inversion method allows us to reconstruct, analysing the dominant part of the seismic signal, both the mechanism and the time history of the seismic source. This is done without constraining the mechanism to be a DC.

Event if we are dealing with a quite noisy area (natural and man made), the method allows us to analyze quite low-energy events ($M<3$) for which, in the frequency interval considered (maximum frequency 10Hz), the point source approximation can be used.

The seismic point source can be mathematically represented by the seismic moment tensor, $M_{ij}(t)$, which is a 3x3 matrix. The ground motion components $u_k(t)$ ($k=1,2,3$) can be written convolving the following elements: the seismic source, i.e. $M_{ij}(t)$; the structural response to sources represented by elementary dipoles with the time dependence given by a δ-function, $G_{k,ij}(t)$; the transfer function of the recording instrument, $R_k(t)$. Formally, it can be written:

$$u_k(t)=\sum_{i,j=1}^{3} M_{ij}(t) * G_{k,ij}(t) * R_k(t) \qquad [1]$$

For a seismic source it is reasonable to consider monotonous time function $M_{ij}(t)$ with an asymptote, i.e. the time derivatives of this function, $\dot{M}_{ij}(t)$, are non-zero in a limited interval only. These time derivatives of the moment tensor components are therefore more convenient for the parametrization than the functions $M_{ij}(t)$ themselves, and it is advantageous to write [1] as:

$$u_k(t)=\sum_{i,j=1}^{3} \dot{M}_{ij}(t) * H_{k,ij}(t) * R_k(t) \qquad [2]$$

where $H_{k,ij}(t)$ are the responses of the medium to sources represented by elementary dipoles with the time dependence given by a Heaviside function.

STRUCTURAL MODEL

The post-caldera activity began 35,000 years ago with the parossistic eruption of the Campanian ignimbrite (sub aerial and chaotic tuffs, followed again by tuffs of submarine environment and local pyroclasts) (Rosi and Sbrana, 1987).

The P-wave velocity distribution has been defined, down to a depth of 3.5 km, using the data recorded inside the Pozzuoli Gulf during a high-resolution reflection seismic survey (Mirabile et al., 1989). From this depth and down to the Moho (about 26 km), deep seismic soundings data have been utilised (Ferrucci et al., 1989). For the upper mantle, the average velocity deduced from surface wave dispersion measurements has been used (Calcagnile and Panza, 1981). The density model has been defined from well measurements and gravimetric inversion (AGIP, 1987), while the Q distribution with depth has been taken as the variable structural parameter in the definition of the structural interpolation range (Sileny', et al., 1992).

The extreme structural models used in the inversion are Pozz1 (Panza et al., 1993) where the shear-wave quality factor Q_s is fixed equal to 100 in the crust and to 200 in the mantle ($Q_p=2.2Q_s$), and Pozz2, which has been obtained from Pozz1 by varying only the values of the quality factor Q (see Table I, and Figure 1), in the superficial layers.

DATA

The 1984 seismic recordings have been made available by the University of Salerno (Department of Physics), while the 1986 data by Aquater (S.p.A.). The instrumental characteristics of the recording stations are shown in Table II (for 1984), and in Table III (for 1986).

The data, filtered with cut-off frequency at 5Hz and 10Hz and resampled with the same time-step of the base functions, have been multiplied with a window D_2 in order to isolate the dominant part of the signal that we want to invert. Such an operation allows us to use that part of the data where the signal to noise ratio is maximum. In the magnitude range considered (see Table IV) the assumption of a point-source is certainly valid when we treat the data filtered at 5Hz; however to obtain an estimate of the stability of the obtained results, it is quite useful to consider higher cut-off frequencies, also for the stronger events.

INVERSION

When inverting the data filtered at 5Hz the number of the triangles, used to parametrize the source time function, varies from 20 to 30, and the base of each triangle is of 0.195 s, while when the cut off frequency is 10Hz, the number of triangles varies from 20 to 40, and each triangle has a base of 0.0976 s. Care must be taken into account while interpreting the final peaks of the source time functions which can be affected by possible structural complexities not considered in the base functions construction (Sileny et al., 1992).

Some of the results of the inversions are shown in the figures from 3 to 8. Each part of each figure is identified by a letter; if this letter is

followed by F, the data considered are the ones filtered with a cut-off frequency at 5Hz; the scale factors are given on the right end side of each part of each figure.

On the base of the hypocentral location (estimated to be 4.3 km from P-wave arrivals, see Table IV) of the event of March 18, 1984, (event N. 7 in Fig. 2) we chose to allow, during the inversion, the hypocentral depth to vary from 3.0 km to 5.5 km, with a step of 0.5 km, (3., 5.5, .5) in Fig. 3 and 4.

The comparison between the two source time functions shows the stability of the inversion, when changing the cut-off frequency (5Hz and 10Hz). The main energy release, occurring at about 0.85 s, can be attributed to the deviatoric part of the seismic moment tensor, and only a small part to the V component (see Fig. 3-4/E-EF). The percentages of the DC, CLVD and V component are given in Table IV.

The average mechanism and that deduced from the first significant peak of the source time function are similar, and in accord with the distribution of the few available clear P-wave polarities.

When the source time function derivative is represented by one triangle of unitary area, the value of M_0 can be determined using the relation given by Silver and Jordan (1982):

$$M_0 = \sqrt{\frac{\sum_{i,j=1}^{3} M_{ij}^2}{2}} \qquad [3]$$

where M_{ij} are the moment rate tensor components. If the source time function f(t), derived from $\dot{M}_{ij}(t)$, is more complex, i.e. it is represented by a series of weighted triangles, the M_0 value is obtained by multiplying right-hand side of [3] with the time integral of f(t):

$$M_0 = \sqrt{\frac{\sum_{i,j=1}^{3} M_{ij}^2}{2}} \int_0^t f(t)\ dt \qquad [4]$$

From the value of M_0 it is possible to obtain the moment-magnitude M_w, following the relation given by Hanks and Kanamori (1979), $M_w = \frac{2}{3} \log_{10} M_0 - 10.7$, if M_0 is expressed in dyne cm, or its equivalent, $M_w = \frac{2}{3} \log_{10} M_0 - 6.0$, (Panza et al., 1993), if M_0 is expressed in N m.

The value of M_w can be compared with the duration magnitude M_d that we have computed for all the events for which sufficiently long records are available to us, using the formula proposed by Esposito et al. (1986) for the P.F. area:

$$M_d = (2.4 \pm 0.07) \log T - (2.1 \pm 0.031) \qquad [5]$$

A summary of these computations is given in Table IV.

From the source time functions of the event occurred on 20 March 1984 (see N. 11 in fig. 2), we can note that the energy release can be divided in two well defined phases: the first energy release occurs around 0.3 s (Fig. 5 D) and it is due to the deviatoric component of the source moment tensor; the second energy release (Fig. 5 E) has a large V component, which characterizes the late part of the whole energy release.

This event, with a large V (explosive) component (30%), seems to start with a deviatoric component, which originates (see Fig. 5 F(f) and G(f)) a strike-slip focal mechanism with a small part of inverse dip-slip. The inverse dip-slip part becomes bigger with increasing time and the V component dominates towards the end of the process (see Fig. 5 F(a) and G(a)). Even if some caution must be taken when interpreting the final energy release dominated by the V component, since it can be generated by structural inadequacy (Sìleny', et al., 1992), the simultaneous presence of V and inverse dip-slip component in the source reveals a possible process of expansion of fluids subsequent to the dislocation.

The total seismic moment deduced from the inversion is $M_0 = 0.08\ 10^{12}$ N m, and consequently $M_w = 1.2$ and $M_d = 1.0$, while if two separate events are considered we have $M_0 = 0.03\ 10^{12}$ N m and $M_0 = 0.05\ 10^{12}$ N m, respectively for the first and the second event, the corresponding M_w being, in the order, 1.0 and 1.1.

The event shown in Figures 6-7 occurred on 31 October 1986 in the area facing the Pozzuoli harbour (event N. 20, Fig. 2). The hypocentral depth estimated, using the P-waves arrivals, 1.9 km, is comparable to the hypocentral depth obtained from our inversion (see Table IV).

The source time function is characterized by a dominant energy release, distributed over a time interval of about 1.0 s (see Figs. 6 CF-DF and 7 CF-DF). Another energy release, smaller than the first, occurs at about 1.8 s. The V component is very low during the whole process.

The comparison between the source time functions of the events N. 11 and N. 20 (whose epicentres are very close each other), recorded in two different periods (1984 and 1986) shows that the V component can vary considerably in time. More specifically, for the 1984 event the V component is near to 30% while for the 1986 one it is less than 5%.

The last event illustrated here in detail, occurred on the 20 September 1986 (event N. 16 in Fig. 2). We allow the hypocentral depth to vary from .25 to 2. km, with a step of 0.25 km (.25, 2., .25) (see Fig. 8).

The seismic moment deduced from our inversion is $M_0 = 0.17\ 10^{12}$ N m, and the moment magnitude is $M_w = 1.5$.

This event contains a relevant V component which characterises the entire rupture process. The deviatoric component is very low and shows a single significant peak centred at 1.2 s, which can be associated to a CLVD (see Table IV).

The analysis of the source time functions represented in Figs. 8 CF-EF shows that there is a first energy release lasting for about 0.8 s generated by a V component, followed by a second release, lasting for about 0.6 s, in which the V and deviatoric components exist simultaneously. The third energy release, lasting for about 1.0 s and essentially associated to a V component must be considered with some caution, since it can be generated by structural inadequacy (Sileny' et al. 1992). The average mechanisms (Figs. 8 FF-GF/(a)) and the mechanisms associated to the first significant energy release (Figs. 8 FF-GF/(f)) show that an explosive dominant process is superimposed to a strike-slip movement. The relevance of the CLVD component ("activation of cracks") indicates the importance that moving fluids can have in the geodynamics of volcanic areas.

A summary of the inversion results for all the events considered is given in Table IV.

There is a very large variability in the percentages of the V component in the source.

The presence of a large V component can be attributed to the inadequacy of the structural models chosen for the inversion. Nevertheless a comparison of the inversion results for the event N. 14 and N. 20 (recorded in 1986), with very similar location, obtained by analysing records from the same four stations (ST07, ST08, ST11, ST13) indicates that real changes of the V component as large as 30% are possible even on time intervals of a few months.

The global trend of the retrieved V, DC, CLVD components for all the analysed events in the P.F. area is shown in figures 9 and 10, respectively for the cases with 5Hz and 10Hz cut-off frequencies. In both cases, in addition to a few events for which the DC component is close to 90% a large number of events is distributed in the central part of the diagrams and therefore the non-DC component in the seismic sources, in the P.F., is significant and can be used to monitor fluid motion in the area.

CONCLUSIONS

When studying seismicity in volcanic areas it is desirable to treat a seismic source in a form a priori not restricted to a DC since its mechanism may reflect not only small scale tectonics but also fluid dynamics. To determine the non DC components of the seismic source it is not possible to use standard methods, based on the distribution of polarities of first arrivals.

The method of waveform inversion that we have developed and applied to a pilot study in the Phlegraean Fields (South Italy) allows us to retrieve the full moment tensor of a point source as a function of time, even when a limited number of records is available. This is particularly important since most of the seismic activity characterizing the studied area is represented by events with relatively low magnitude, in the range from 1 to 3. When a seismic crisis occurs, usually in connection with bradeysism, the number of these events is very large, and our method gives the possibility to study the seismic moment tensor of three all of them and, therefore to extract statistically significant information about the local stress field.

In comparison with already existing similar approaches, the method presents the following main advantages: 1) the information about the focal mechanism is obtained utilizing a very small number of records, i.e. a minimum of four station is sufficient, resolving in this way the problem, frequently present, of the unavailability of a very dense local network; 2) the focal mechanism is determined from the inversion of the dominant part of the seismogram and not only from the inversion of single phases of the seismogram. This is particularly important in volcanic areas, where the high level of noise makes extremely difficult, if not impossible, the correct reading of the polarity of the first arrivals and the isolation of single phases; 3) it allows to vary the structural model and the source depth during the inversion, reducing the effect of the structural inadequacy and of a wrong hypocentral location on the retrieved focal mechanisms and source time function.

Even if the retrieved percentages of non-DC components can be affected by structural inadequacy, it is possible to detect real changes in time of these percentages, by analysing events with very similar epicentral locations. The monitoring of the time variation of the non-DC component (CLVD and V components) can be used to monitor possible fluid motion, which can be a precursor to eruptions.

ACKNOWLEDGEMENTS

We thank Aquater S.p.A. and Prof. Del Pezzo for making available the data collected in the Pozzuoli area. We thank Dr. Sileny' for many valuable suggestions and for critically reading the manoscript. We acknowledge financial support from GNDT (CNR grants # 90.01007.54 and 91.02539.54) and MURST (40% and 60% Funds). Special thanks go to ENEA for allowing us the use of the IBM 3090E of the Computer Centre ENEA INFO BOL. The research has been carried out in the framework of the activities planned by the Central European Initiative - Committee for Earth Sciences, and is a contribution of the ILP Task Group II-4.

REFERENCES

AGIP, 1987. *Geologia e geofisica del sistema geotermico dei* Campi Flegrei. MESG-SERG, S. Donato Milanese, 1-19.

Barberi F., Carapezza M., Innocenti F., Luongo G. and Santacroce R., 1989. *The problem of volcanic unrest: The* Phlegraean Fields *case history*. In: A. Boriani M. Bonafede G.B. Piccardo & G.B. Vai (ed.), *The lithosphere in Italy: advances in earth science research*. Atti Conv. Lincei, 80, 387-406, Accademia Nazionale dei Lincei, Roma.

Calcagnile G. and Panza G.F., 1981. *The main characteristics of the lithosphere-asthenosphere system in Italy and surrounding regions*. Pure Appl. Geophys., 119, 865-879.

Esposito E., Luongo G., Marturano A., Porfido S., Ricciardi G.P., 1986. *Relazione magnitudo-intensità per i Campi Flegrei*. Bollettino G.N.V. - C.N.R., 227-233.

Ferrucci F., Gaudiosi G., Hirn A., Luongo G., Mirabile L., Pino N.A., 1989. *Seismic detection of a major upheaval beneath the* Campania *volcanic area (Naples, southern Italy)*. Geophys. Res. Lett., 16, 1317-1320.

Hanks T.C. and Kanamori H., 1979. *A moment-magnitude scale*. J. Geophys. Res., 84, 2348-2350.

Jost M.L., Herrmann R.B., 1989. *A student's guide to and review of moment tensors*. Seismological Research Letters, 60, 2.

Mirabile L., Nicolich R., Piermatte R. and Ranieri G., 1989. *Identificazione delle strutture tettono-vulcaniche dell'area Flegrea: sismica multicanale nel golfo di* Pozzuoli. Atti VII Conv. GNGTS, Vol. II, 829-838.

Panza G.F., Sìleny' J., Campus P., Nicolich R. and Ranieri G., 1993. *Point source moment tensor retrieval in volcanic, geothermal and orogenic areas by complete waveform inversion*. Int. J. Appl. Geophys., 30, 98-118.

Rosi M., Sbrana A., 1987. *Phlegraean Fields*. CNR. Quaderni della ricerca scientifica, 114, pp. 175.

Sìleny' J. and Panza G.F., 1991. *Inversion of seismograms to determine simultaneously the moment tensor components and source time function for a point source buried in a horizontally layered medium*. Studia Geophysica et Geodaetica, 35, 166-183.

Sìleny' J., Panza G.F., Campus P., 1992. *Waveform inversion for point source moment tensor retrieval with variable hypocentral depth and structural model*. Geophys. J. Int., 109, 259-274.

Silver P.G. and Jordan T.H., 1982. *Optimal estimation of scalar seismic moment*. Geophys. J. R. Astr. Soc., 70, 755-787.

TABLE CAPTIONS

TABLE I Q-values used in the structures relative to the Pozzuoli area.

TABLE II Instrumental characteristics and coordinates of the recording stations of the network used in 1984.

TABLE III Instrumental characteristics and coordinates of the recording stations of the network used in 1986.

TABLE IV Summary of all the performed inversions. n is the order number of the event; date, origin time, epicentral location and hypocentral depth (h) are obtained using Hypo71 program. In the following columns the result of the waveform inversion is shown. Depth indicates the inverted hypocentral depth. Lower case letters a and b indicate, respectively, the result obtained inverting data filtred with a cut-off frequency at 5Hz and 10Hz data. In the last column the duration magnitude (M_d) is shown, as determined from the few records available with sufficient length for such a measure. The other empty fields indicate the cases in which the signal/noise ratio in the data does not warrant their inversion.

TABLE I

Thickness of the layer(s) (km)	Q_s	Q_p
Structure Pozz1		
24.45	100	220
Mantle	200	440
Structure Pozz2		
0.95	25	55
2.90	50	110
20.60	100	220
Mantle	200	440

TABLE II

Station identific N	Geophone type	Magnification (mV/cm·s⁻¹)	Period (s)	Damping ratio	Latitude (40°N)	Longitude (14°E)
W 03	Wisconsin	3658	0.77	0.18	50.77'	09.17'
W 04	Wisconsin	3658	0.77	0.18	50.11'	05.03'
W 10	Wisconsin	3658	0.77	0.18	46.69'	05.37'
W 11	Wisconsin	3658	0.77	0.18	49.26'	07.25'
W 12	Wisconsin	3658	0.77	0.18	49.60'	08.66'
W 14	Wisconsin	3658	0.77	0.18	47.78'	09.90'
W 15	Wisconsin	3658	0.77	0.18	49.51'	09.84'
W 20	Wisconsin	3658	0.77	0.18	51.14'	05.89'
W 21	Wisconsin	3658	0.77	0.18	50.47'	07.67'

TABLE III

Station identific N	Geophone type	Magnification (V/cm·s⁻¹)	Period (s)	Damping ratio	Latitude (40°N)	Longitude (14°E)
ST 07	S 13	8	1.0	80	49.46'	04.40'
ST 08	S 13	16	1.0	80	51.14'	05.89'
ST 11	S 13	16	1.0	80	47.82'	09.63'
ST 13	S 13	4	1.0	80	50.47'	08.28'

TABLE IV

N	Date (d m y)	Origin time (h m s)	Location Lat. (40°N)	Location Long. (14°E)	h (km)	Depth (km) a	Depth (km) b	V (%) a	V (%) b	CLVD (%) a	CLVD (%) b	DC (%) a	DC (%) b	M_0 (10^{12} N·m) a	M_0 (10^{12} N·m) b	M_w a	M_w b	M_d
1	15 03 84	21 24 41.73	48.98'	07.92'	6.8	7.1	7.4	30	15	15	30	55	55	7.27	10.9	2.5	2.7	–
2	15 03 84	23 05 59.51	50.83'	08.69'	3.0	2.0	2.4	15	15	30	25	55	60	0.10	0.33	1.3	1.7	1.3
3	16 03 84	08 08 58.51	50.02'	07.35'	3.0	1.7	–	25	–	10	–	65	–	0.21	–	1.5	–	1.7
4	18 03 84	17 46 43.90	48.14'	06.52'	4.5	3.6	3.5	5	5	10	10	85	85	41.1	40.5	3.0	3.0	–
5	18 03 84	17 54 22.75	48.58'	04.87'	4.2	3.0	3.0	0	5	0	5	100	90	0.26	0.24	1.6	1.6	–
6	18 03 84	19 54 49.29	50.21'	06.49'	0.2	1.6	1.5	15	20	30	30	55	50	0.06	0.05	1.2	1.1	1.3
7	18 03 84	20 29 35.24	48.98'	07.92'	4.3	3.3	3.7	10	10	20	20	70	70	3.30	3.80	2.3	2.4	2.2
8	19 03 84	01 31 53.99	48.22'	07.26'	3.5	2.0	2.0	0	15	0	20	100	65	0.14	0.14	1.4	1.4	1.9
9	19 03 84	13 47 48.50	49.70'	08.76'	0.7	0.6	1.8	10	10	10	35	80	55	0.01	0.04	0.6	1.0	1.3
10	19 03 84	16 46 22.93	50.07'	09.06'	3.4	2.5	–	30	–	15	–	55	–	0.42	–	1.7	–	–
11	20 03 84	11 47 27.10	48.94'	07.35'	1.7	1.4	1.7	15	30	35	10	50	60	0.02	0.08	0.9	1.2	1.0
12	20 03 84	21 21 34.03	49.21'	04.74'	3.7	2.5	2.5	5	30	5	15	90	55	0.06	0.09	1.2	1.3	1.7
13	20 03 84	23 42 44.82	48.17'	05.72'	3.0	2.9	–	5	–	5	–	90	–	0.08	–	1.3	–	1.6
14	28 07 86	23 16 41.75	49.19'	07.02'	1.0	1.0	1.3	20	30	5	20	75	50	0.03	0.25	1.0	1.6	–
15	20 09 86	23 17 50.45	49.49'	05.17'	0.8	1.5	1.0	5	30	25	30	70	40	0.25	0.24	1.6	1.6	–
16	20 09 86	23 35 56.64	49.50'	05.17'	0.9	1.8	1.1	30	25	25	15	45	60	0.17	0.13	1.5	1.4	–
17	08 10 86	01 38 03.59	49.43'	06.62'	0.4	–	1.0	–	0	–	5	–	95	–	0.06	–	1.2	–
18	11 10 86	02 22 29.24	49.33'	05.17'	1.0	2.0	1.2	20	25	20	20	60	55	0.55	0.49	1.8	1.8	–
19	26 10 86	00 12 07.09	48.85'	08.31'	1.0	1.3	1.9	15	20	35	25	50	55	0.50	1.50	1.8	2.1	–
20	31 10 86	03 51 29.08	49.01'	06.92'	1.9	2.0	2.2	5	0	15	5	80	95	0.30	0.75	1.6	1.9	–
21	09 11 86	01 21 00.71	49.65'	05.68'	0.4	0.7	1.7	0	15	10	30	90	55	0.16	0.23	1.4	1.5	–

FIGURE CAPTIONS

Fig. 1: Structural models, for the Phlegraean Fields, used in this study.

Fig. 2: Seismographic network and epicentral distribution: W followed by a number indicates the stations we have considered to study the 1984 events, ST followed by a number indicates the station considered to study the 1986 events, open circles indicate 1984 epicentres, full circles indicate 1986 epicentres.

Fig. 3: Event of March, 18, 1984 (number 7 in Table IV); data and base functions have a maximum frequency of 5 Hz. AF): Real data: continuous line; synthetic data: dashed line. The identification of each station and the values of the maximum amplitudes expressed in mVolts are given in the figure. BF) The continuous line represents the time dependence of the six elements (F1,....., F6) of the first time-derivative of the seismic moment tensor; the dashed line represents the time dependence of their deviatoric part. CF) Common shape of the six elements of the first time-derivative of the moment tensor. DF) Deviatoric part of the first time-derivative of the moment tensor. EF) The V part of the first time-derivative of the moment tensor is shown. FF) Focal mechanisms associated to the complete seismic moment tensor; (a) indicates the average mechanism which characterizes the entire energy release, while (f) indicates the mechanism obtained

from the "first significant peak" chosen, indicated with (*) in part C of the figure. GF) Focal mechanism corresponding to the deviatoric part of the seismic moment tensor. In parts FF) and GF) of the figures the shaded zones indicate areas of compression and white zones areas of dilatation; the two great circles identify the best DC (Jost and Herrmann, 1989) consistent with the inversion, and full circles indicate positive P-waves polarities, while open circles indicate negative P-wave polarities.

Fig. 4: Event of March, 18, 1984 (number 7 in Table IV); data and base functions have a maximum frequency of 10 Hz. The figures are indicated with the letters from A) to G). For the description, see Fig. 3.

Fig. 5: Event of March, 20, 1984 (number 11 in Table IV); data and base functions have a maximum frequency of 10 Hz. The figures are indicated with the letters from A) to G). For the description, see Fig. 3.

Fig. 6 Event of October, 31, 1986 (number 20 in Table IV); data and base functions have a maximum frequency content of 5 Hz. AF) Real data: continuous line; synthetic date: dashed line. The identification of each station and the values of the maximum amplitudes expressed in Volt are given in the figure. BF) The continuous line represents the time dependence of the six elements (F1,....., F6) of the the first derivative of the seismic moment tensor; the dashed line represents the time dependence of their deviatoric part. CF) Common shape of the six elements of the first time-derivative of the moment tensor. DF) Deviatoric part of the first time-derivative of the moment tensor. EF) The V part of the the first time-derivative of the moment tensor are shown. FF) Focal mechanisms associated to the complete seismic moment tensor; (a) indicates the average mechanism which characterizes the entire energy release, while (f) indicates the mechanism obtained from the "first significant peak" chosen, indicated with (*) in part C of the figure. GF) Focal mechanism corresponding to the deviatoric part of the the first derivative of the seismic moment tensor. In parts FF) and GF) of the figures the shaded zones indicate areas of compression and white zones areas of dilatation; the two great circles identify the best DC (Jost and Herrmann, 1989) consistent with the inversion, and full circles indicate positive P-waves polarities, while open circles indicate negative P-wave polarities.

Fig. 7: Event of October, 31, 1986 (number 20 in Table IV); data and base functions have a maximum frequency of 10 Hz. The figures are indicated with the letters from A) to G). For the description, see Fig. 6.

Fig. 8: Event of September, 20, 1986 (number 16 in Table IV); data and base functions have a maximum frequency of 5 Hz. The figures are indicated with the letters from AF) to GF). For the description, see Fig. 6.

Fig. 9 Percentages of V, CLVD and DC obtained from the inversion of the data filtred with a cut-off frequency at 5Hz. The numbers correspond to the order number of the epicentres shown in Fig. 2 and listed Table IV.

Fig. 10 As in Fig. 9, but with cut-off frequency at 10Hz.

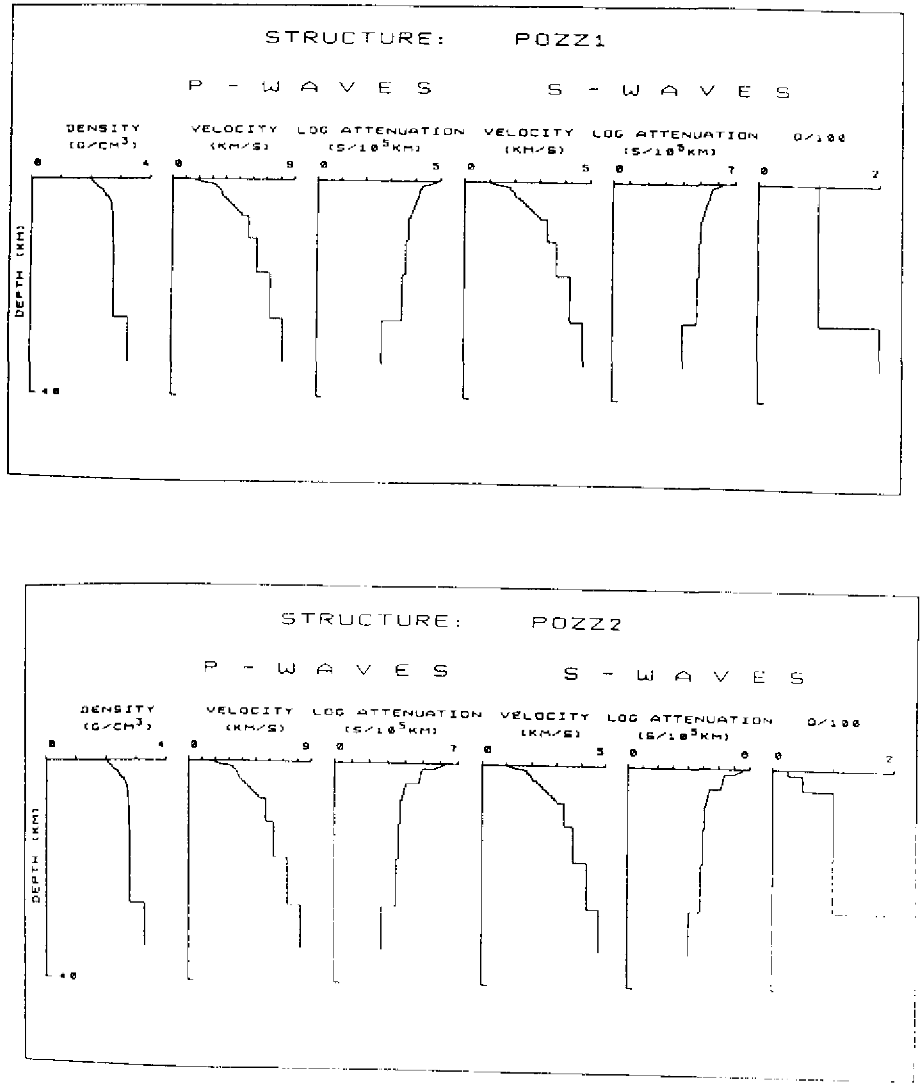

Fig.1

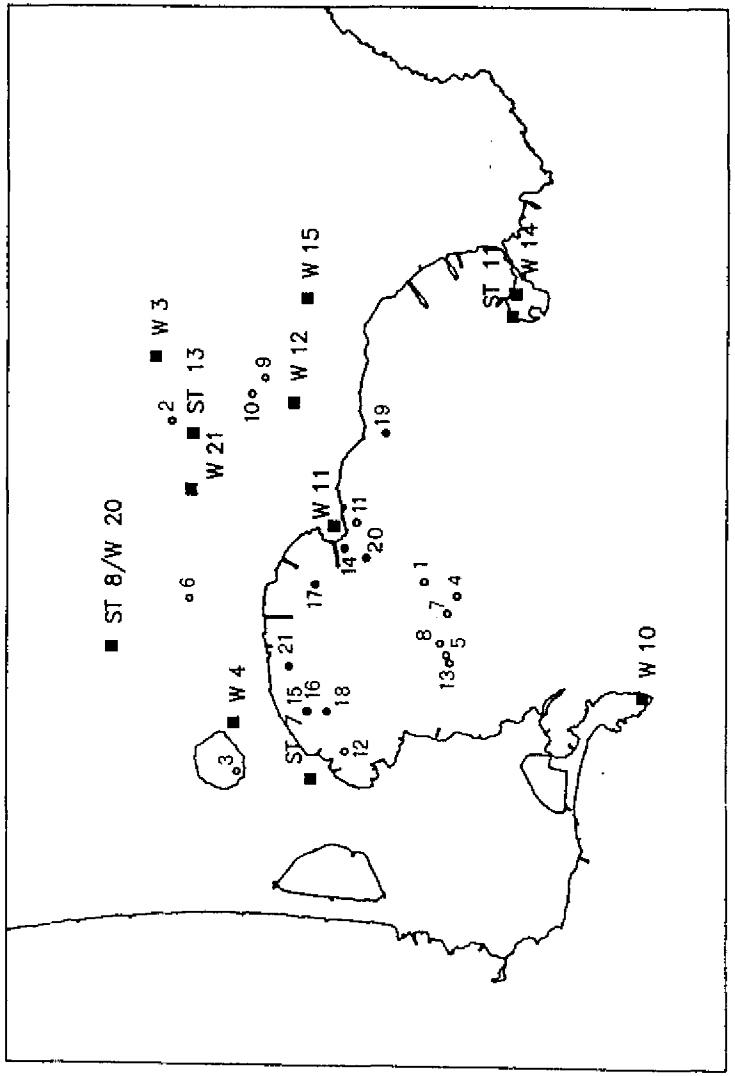
PHLEGREAN FIELDS
1984/86
SCALE 1/50000
ST 8/W 20
W 3
W 4
W 10
W 11
W 12
W 14
W 15
W 21
ST 11
ST 13
ST

Fig.2

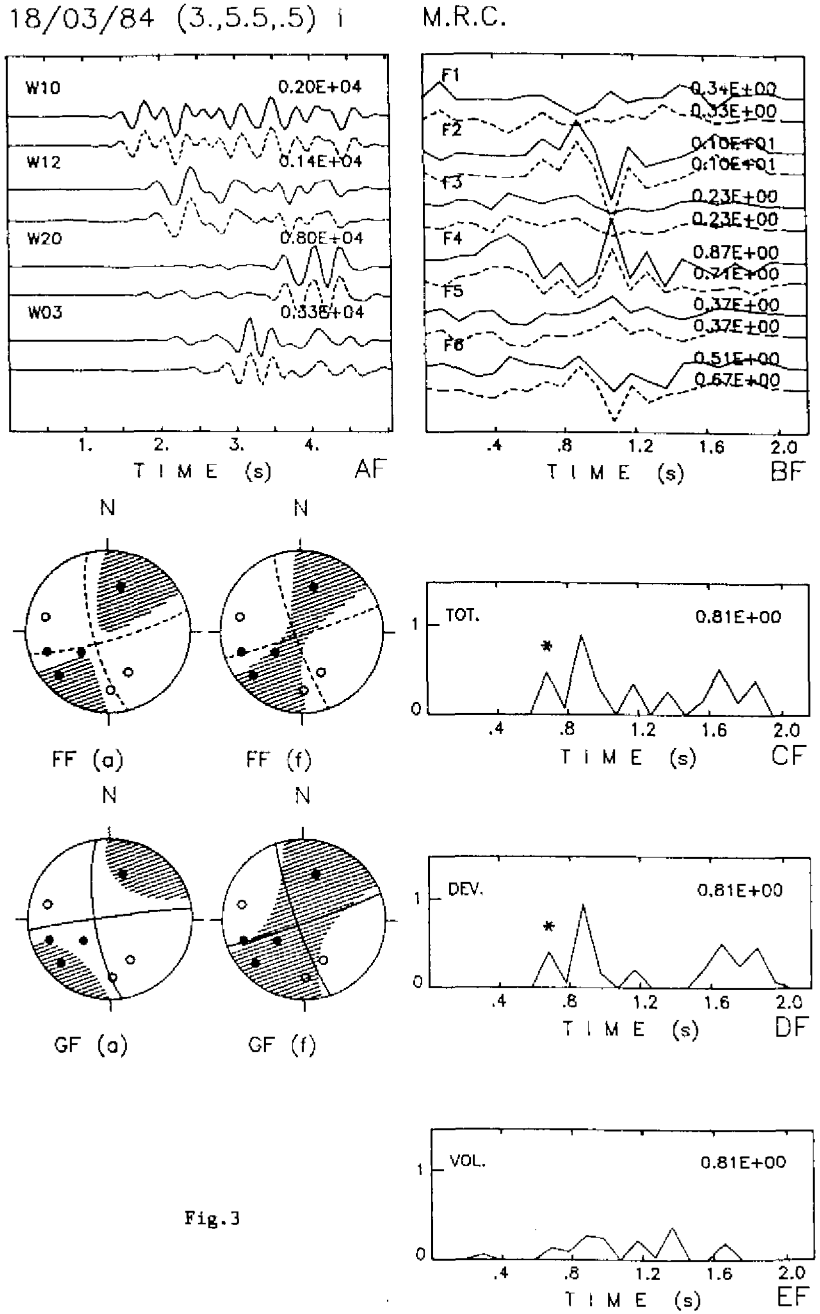
18/03/84 (3.,5.5,.5) i
M.R.C.
W10
0.20E+04
W12
0.14E+04
W20
0.80E+04
W03
0.33E+04
TIME (s)
AF
F1
F2
F3
F4
F5
F6
TIME (s)
BF
N
FF (a)
FF (f)
TOT.
0.81E+00
TIME (s)
CF
GF (a)
GF (f)
DEV.
0.81E+00
TIME (s)
DF
VOL.
0.81E+00
TIME (s)
EF

Fig.3

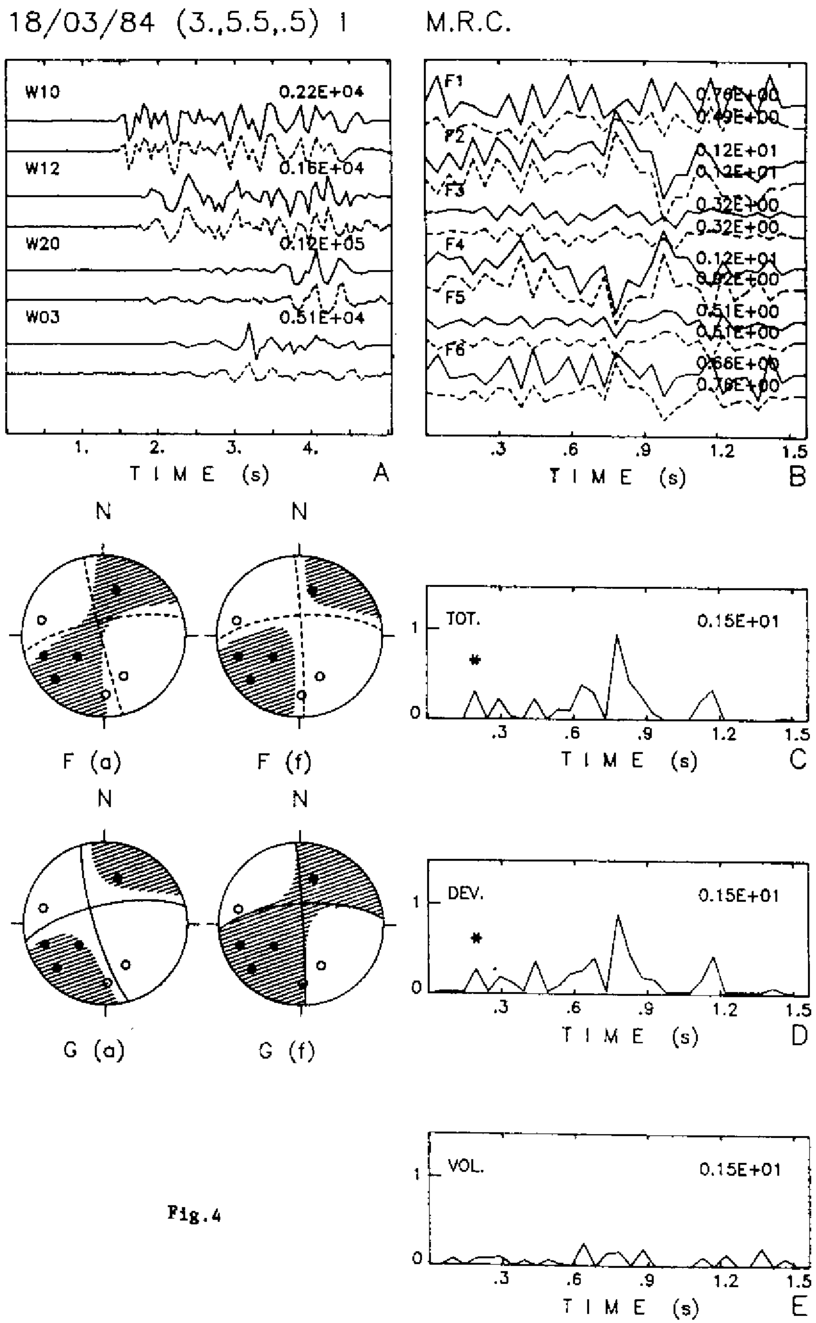
18/03/84 (3.,5.5,.5) 1
M.R.C.
W10 0.22E+04
W12 0.16E+04
W20 0.12E+05
W03 0.51E+04
TIME (s)
A
B
F (a)
F (f)
G (a)
G (f)
TOT. 0.15E+01
DEV. 0.15E+01
VOL. 0.15E+01
C
D
E

Fig.4

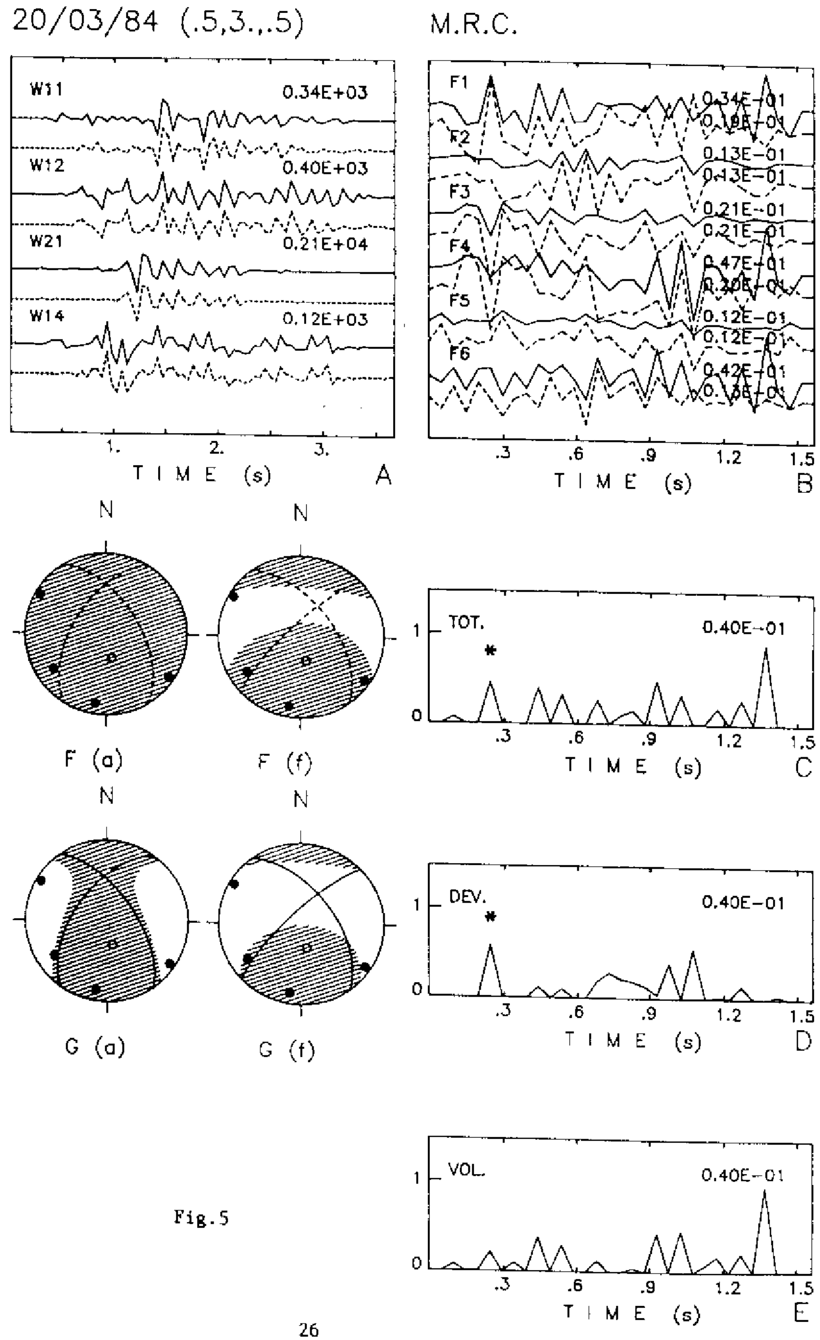
20/03/84 (.5,3.,.5)
M.R.C.
W11 0.34E+03
W12 0.40E+03
W21 0.21E+04
W14 0.12E+03
TIME (s)
A
B
F (a)
F (f)
G (a)
G (f)
TOT. 0.40E-01
DEV. 0.40E-01
VOL. 0.40E-01
C
D
E

Fig.5

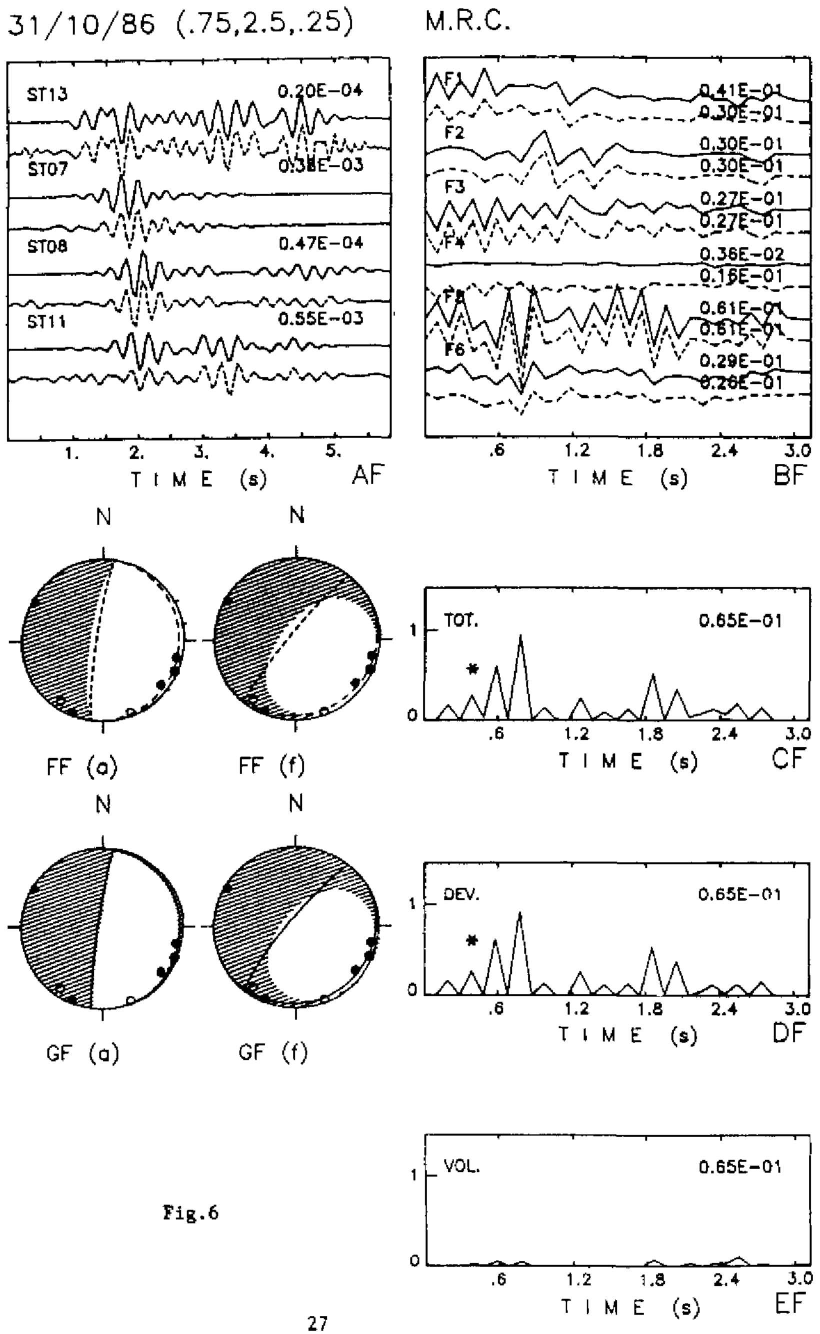
31/10/86 (.75,2.5,.25)
M.R.C.
ST13
0.20E-04
ST07
0.38E-03
ST08
0.47E-04
ST11
0.55E-03
T I M E (s)
AF
F1
F2
F3
F4
F5
F6
0.41E-01
0.30E-01
0.30E-01
0.30E-01
0.27E-01
0.27E-01
0.36E-02
0.16E-01
0.61E-01
0.61E-01
0.29E-01
0.28E-01
T I M E (s)
BF
N
FF (a)
FF (f)
TOT.
0.65E-01
CF
GF (a)
GF (f)
DEV.
0.65E-01
DF
VOL.
0.65E-01
EF

Fig.6

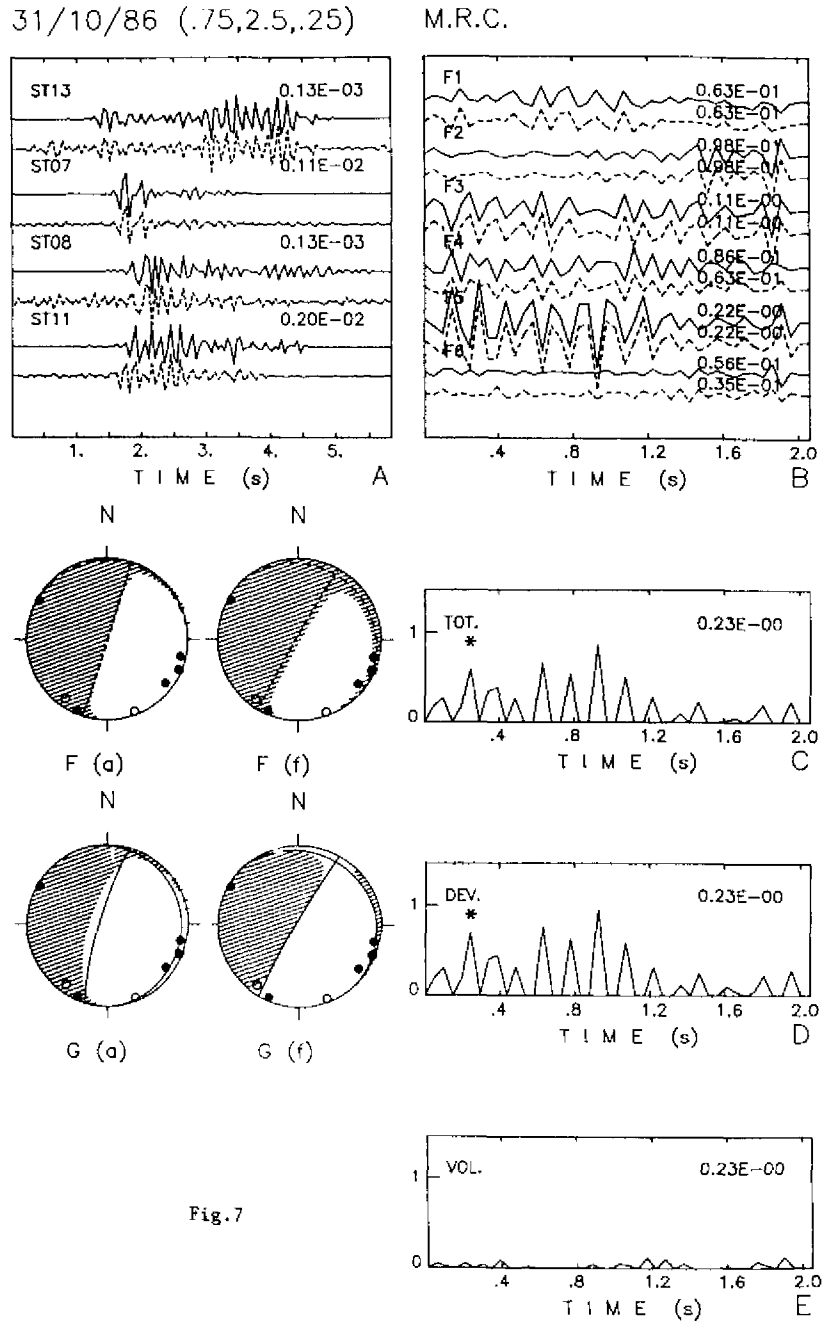
31/10/86 (.75,2.5,.25)
M.R.C.
ST13
0.13E-03
ST07
0.11E-02
ST08
0.13E-03
ST11
0.20E-02
T I M E (s)
A
F1
F2
F3
F4
F5
F6
0.63E-01
0.63E-01
0.98E-01
0.98E-01
0.11E-00
0.11E-00
0.86E-01
0.63E-01
0.22E-00
0.22E-00
0.56E-01
0.35E-01
T I M E (s)
B
N
F (a)
F (f)
TOT.
0.23E-00
C
G (a)
G (f)
DEV.
0.23E-00
D
VOL.
0.23E-00
E

Fig.7

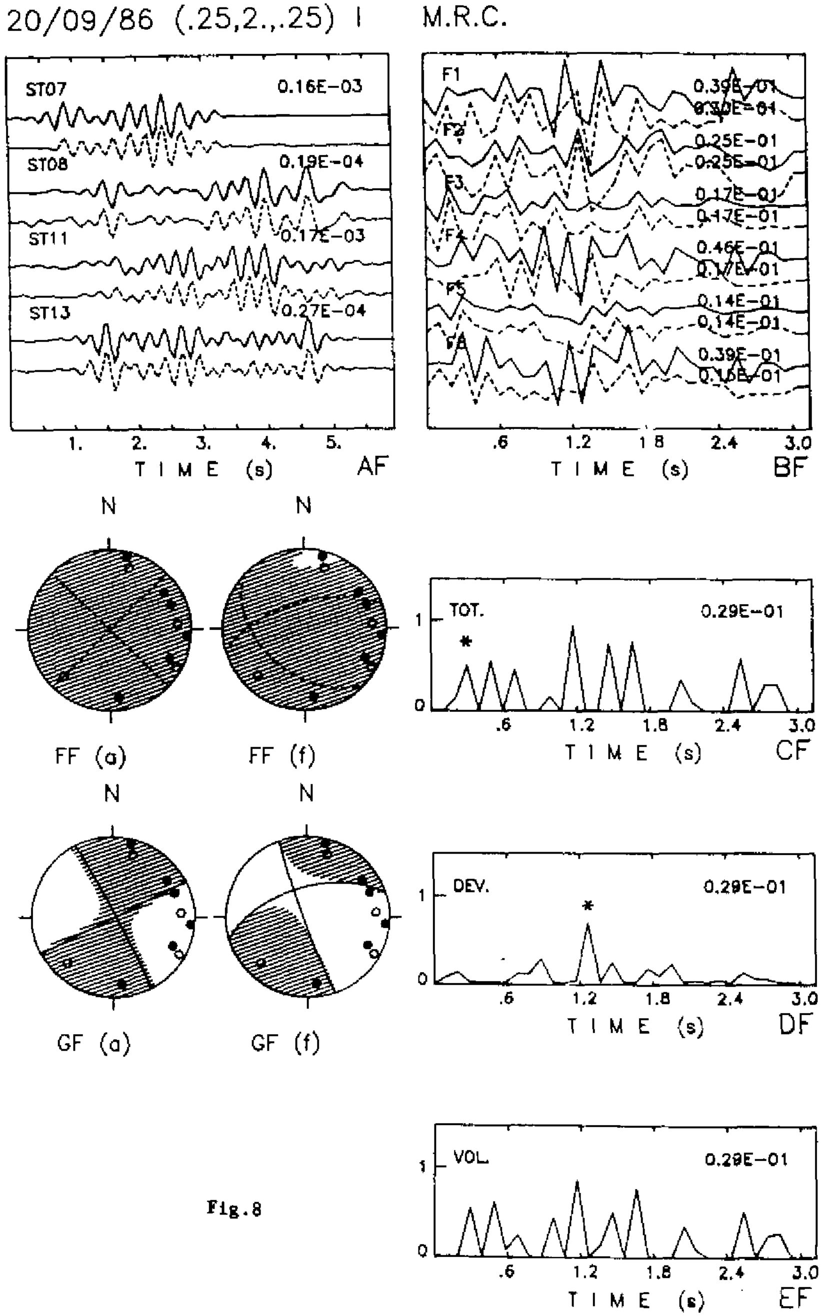
20/09/86 (.25,2.,.25) I
M.R.C.
ST07
0.16E-03
ST08
0.19E-04
ST11
0.17E-03
ST13
0.27E-04
TIME (s)
AF
F1
F2
F3
F4
F5
F6
TIME (s)
BF
N
FF (a)
FF (f)
GF (a)
GF (f)
TOT.
0.29E-01
TIME (s)
CF
DEV.
0.29E-01
TIME (s)
DF
VOL.
0.29E-01
TIME (s)
EF

Fig.8

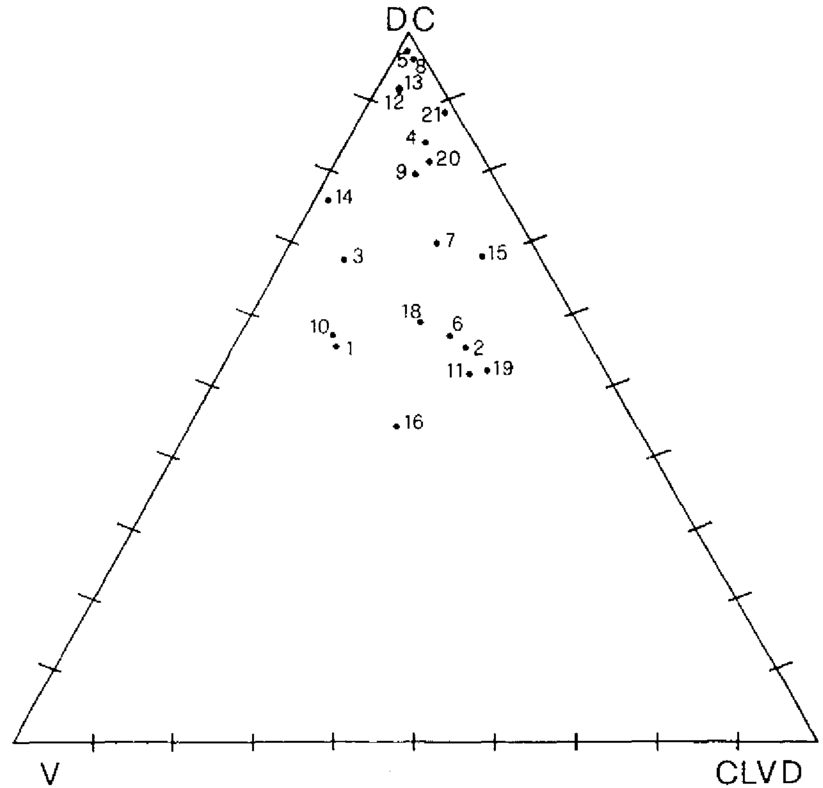
DC
V
CLVD

Fig.9

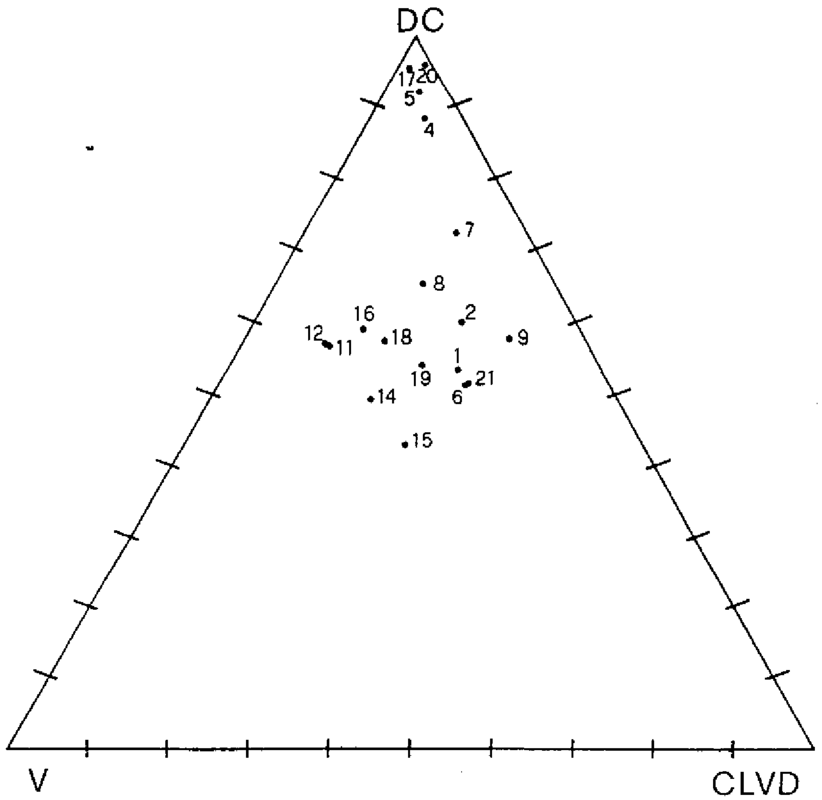

Fig.10